Proc. of the International Conference on Electrical, Computer, Communications and Mechatronics Engineering (ICECCME 2024)
4-6 November 2024, Male, Maldives

Overhead Transmission Line Temperature Estimation Based on Artificial Neural Networks

Emanuele Ogliari
Department of Energy
Politecnico di Milano
Milan, Italy
emanuelegiovanni.ogliari@polimi.it

Roberto Sebastiano Faranda
Department of Energy
Politecnico di Milano
Milan, Italy
roberto.faranda@polimi.it

***Abstract*—To ensure the power system operates optimally and economically, precise evaluations of component physical limitations are necessary. Hence, to evaluate these constrains, electrical grid operators usually adopt well-known methods based on mathematical model which better describe the physics behaviour of the system. An effective approach to estimate these limits is here presented employing Artificial Neural Network (ANN). With traditional methods, these estimations could be inaccurate due to many factors. Therefore, in this work an ANN based method to estimate all the working temperatures of overhead transmission lines has been presented. The estimation of the proposed ANN based method is compared to the CIGRE physical model. The case study results, based in real data, clearly show the great applicability and the improved accuracy of this proposed ANN based method.**

Keywords—DTR, Thermal estimation, CIGRE thermal model, IEEE thermal model, ANN model, Overhead line

I. INTRODUCTION

Due to the growing number of loads and Renewable Energy Sources (RES) generators connected to the power grid, Transmission System Operator (TSO) often face congestion issues: it is thus necessary to increase the exploitable line capacity. In most of cases, not having any available real measurement in the line section where the congestion occurs, capacity limits are often estimated through indirect methods. Obviously, the use of conservative calculations, often underestimating the actual capacity available under certain conditions, leads to improper decision in terms of optimization of power system operation, such as absorbed load reduction, generation reduction and interventions on entire lines.

To address this, expanding the capacity of transmission and distribution lines, such as through infrastructure upgrades, is a fundamental solution. However, some limitations exist as: high costs, steep population density growth, intensive usage of lands for various developments and legal difficulties of building new lines. To increase transmission line capacity more cost-effectively, grid operators are primarily focusing on strategies that accurately assess thermal limits. These strategies must ensure reliability and safety while maintaining adequate line clearances, avoiding the need for time-consuming line annealing [1].

This study was carried out within the MUSA – Multilayered Urban Sustainability Action (ECS 00000037) – project, funded by the European Union – Next-Generation EU, under the National Recovery and Resilience Plan (NRRP) Mission 4 Component 2 Investment Line 1.5: Strengthening of research structures and creation of R&D "innovation ecosystems", set up of "territorial leaders in R&D". This manuscript reflects only the authors' views and opinions, neither the European Union nor the European Commission can be considered responsible for them.

Maximum power transfer in transmission lines is fixed and based on three limits: stability, thermal and mechanical. Stability limit commonly restricts the maximum power for high voltage and long transmission lines, and it depends on the line impedance. Thermal limit is a constraint referring to the losses both of thermal and mechanical properties of the conductor because of overheating. Mechanical limit applies for OverHead Lines (OHLs) and it is defined by the minimum distance between conductor and ground; this usually limits the current intensity for short and medium OHLs.

In this contest, one of the most promising methods to increase the capacity of an existing transmission line is the Dynamic Thermal Rating (DTR) [2]-[5], where the term *thermal rating* represents the value of the continuous conductor current which would produce the maximum allowable conductor temperature in a specific location and time along a power transmission line [6]. This current level is known as the *ampacity* of the line, and it can be used as a static or dynamic value [7]. According to this main classification, the relevant estimation models found in literature can be different, as detailed in Fig. 1 [8] and [9].

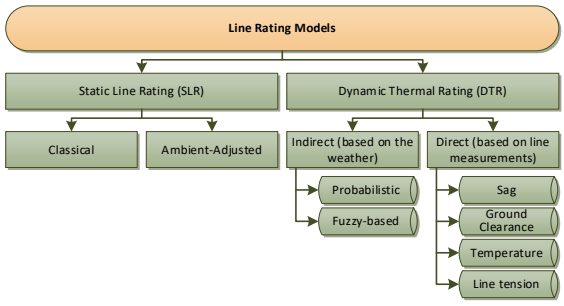

Fig. 1. Main models grouping according to the line thermal rating

Table I [10] qualitatively summarizes the effect of weather fluctuations or changes on thermal ratings of a current carrying conductor.

TABLE I
QUALITATIVE EFFECT OF WEATHER CHANGES ON THERMAL RATINGS FOUND IN THE BIBLIOGRAPHIC REVIEW

Climatic factor	*Variation*	*Conductor capacity*
Ambient air temperature	2% actuation 10% decrease	±2% +11%
Wind speed and direction	1 m/s increase 90° angle	≈18% ≈23%
Solar radiation	Cloud shadowing total eclipse	±a few percent +18%

Therefore, considering an OHL, it is evident that both climatic/weather factors and conductor features has a very strong effect on DTR estimation. Besides, it has been

demonstrated that physical methods are largely affected by inaccuracies of input data, when employed as forecasting models as the weather forecasts are often inaccurate. Moreover, Machine Learning (ML) based model have been successfully employed when the modelled system was too complex and, due to their data driven logic, have proved to be noise independent i.e. are capable of mitigating the weather forecasts error by learning its trend.

Finally, in this paper, results of the Dynamic Thermal Rating based on CIGRE model, which is currently adopted by a TSO and an Artificial Neural Network (ANN) based method are compared with measured values of existing overhead lines temperature. In the temperature estimation with the physical model, transient overload is exploited.

II. Dynamic Thermal Line Rating

Dynamic Thermal Line Rating (DTR) can increase the estimation accuracy of ampacity of existing transmission lines [5] by dynamically adjusting the line temperature estimation. Dynamic ampacity, usually called Dynamic Line Rating (DLR), is based upon actual weather and pre-load conditions (rather than worst case ones) [11] and is thus normally higher than static ratings. For some applications real-time field monitoring is required, continual re-calculation of thermal ratings and it considers the variability of the line characteristics along with its surroundings [12] and [13]. The real-time monitoring of electrical systems and environmental parameters can help to dynamically rate transmission lines and thus helps in maximizing the thermal capacity of critical OHLs. Weather variation can greatly influence the ampacity of the lines. In [8]-[10] it is studied the effect of weather fluctuations on thermal ratings of a current carrying conductor, highlighting the relevance of wind variation, line angle and convective cooling on conductor capacity, in lightly loaded lines.

In most of the cases, DLR implementation provides additional transmission capacity with respect to static line ratings, reducing the curtailments and the rate of line congestion. This issue has been proved to be particularly important for wind energy integration in proximity of the wind power plant itself.

When the energy production is high, the OHL is subjected to an important cooling effect due to the wind, increasing the line ampacity with respect to the static limits [14] and the transmission capacity [15]. Associated risks to the adoption of DLR are mainly related to thermal aging and spatial and temporal variability of the ampacity. In addition, the implementation of dynamic line rating requires the availability of accurate predictions and/or measurements of environmental and structural parameters. As detailed in Fig. 1, there are two main approaches to provide DLR, Direct and Indirect Methods [7] and [16]. In this work to know the conductor temperature on a span Direct Method (measure), Indirect Physical method and Indirect ANN method will be considered. In particular, the line temperature is measured, and a comparison is executed on four reals Italian OHLs every 5-minutes-ahead.

Indirect Physical Method

Indirect methods of DLR estimation, is a prediction-based data which uses weather data from the weather stations or generating data by using numerical weather modelling. To calculate the ampacity of the OHL under given weather conditions, the heat balance equation (1), together with industrial standard-based component thermal models, is adopted.

$$mc \cdot \frac{dT_{line}}{dt} = P_j + P_s - P_c - P_r \quad (1)$$

where mc is the thermal capacity of the line per unit of length, T_{line} is the line temperature, P_j and P_S are the heating components related to joule losses and solar irradiation and P_C and P_r are the cooling components referred to convection and radiation. Some of the methodologies that are being used to calculate thermal rating of OHLs are standards reported by IEEE and CIGRE [17] and [18]. With these methodologies, line capacity should be estimated for each span and then the minimum value should be kept. Alternatively, a sensitivity analysis must be conducted to identify the critical spans where that methods will be then applied. The two methods differ in how they account for the effects of forced and natural convection.

The CIGRE standard employs empirical correlations to calculate natural convection, using Grashof and Prandtl numbers. Forced convection is determined primarily through the Nusselt number. The standard suggests considering forced convection for wind speeds above 0.5m/s and choosing the dominant value for lower velocities. Further empirical correlations are proposed. The user guide for CIGRE adoption, additionally, highlights that, considerable errors can occur in case of high wind speeds, due to the difficulty in assessing turbulent behaviour of air, indeed, the validity limit for the above-mentioned correlations is set at Reynold number equal to 4000 [19].

In contrast to the CIGRE model, the IEEE provides two relationships both for high and low wind speeds, considering Nusselt coefficient and the wind direction. For natural convection, an empirical equation based on several parameters as: conductor diameter, air density and temperature difference, is used. The model recommends selecting the higher value from the two forced convection relationships for wind speeds exceeding 0.2 m/s and considering natural convection for lower velocities. The acceptable range of variation of the wind speed is from 0m/s to 18.9m/s [20].

The main advantage of these methodologies is related to the low installation cost of the required equipment and the possibility to perform it without any outage of the line. To get the required meteorological measurements conductor replicas, weather stations or Numerical Weather Prediction (NWP) models can be adopted[1]. These techniques are particularly suitable for lightly loaded lines, where the current density is lower than 0.5A/mm^2 [20].

Indirect ANN Method

ANN are ML techniques that model the structure and learning process of the human brain. The ANN architecture typically consists of three layers: an input layer, one or more hidden layers, and an output layer. The input layer receives external data, which is then processed by hidden neurons in the hidden layers. Finally, the output layer generates predictions based on the information from the previous layers. ANNs excel at approximating complex, nonlinear

[1] Numerical Weather Prediction (NWP) models focus on taking current observations of weather and processing these data with computer-based models to forecast the future state of weather.

relationships between input and output data with high accuracy.

A schematic representation of a feed-forward ANN with a double hidden layer is reported in Fig. 2. The term "feed-forward" means that the data move only in forward direction, from input to output nodes, without any feedback connection between layers. Each layer is composed by artificial neurons, basic processing units also called "perceptrons" or "nodes". Different neurons are connected to each other by means of weighted connections. Positive weights determine excitatory connections, while negative weights characterize inhibitory connections. Each unit performs a relatively simple job: it receives inputs from neighbours or external sources and use them to compute an output signal which is propagated to other units [21].

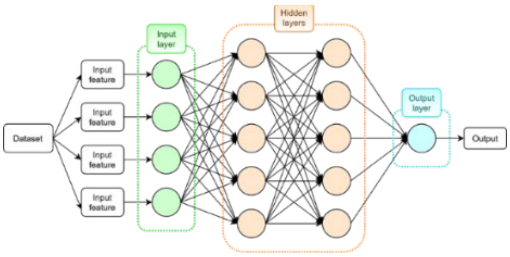

Fig. 2. Schematic of a feed-forward ANN with a double hidden layer

An ANN learns an internal representation of the existing relations between input and output by means of the training procedure. During this process, the optimal weight of each connection between neurons is selected. Training is usually performed in a supervised manner, meaning that both input and the corresponding desired output are delivered to the algorithm. First, the weights are randomly set. Then, the examples are presented to the network one by one. For every example presented, an error metric is used to quantify the difference between provided and desired output. Weights and biases are adjusted in such a way to minimize the error computed. To achieve good generalization capabilities from the process, a suitable training algorithm must be selected.

One of the problems occurring during ANN training process is the so-called overfitting. In detail, the error on the training set drops to very small values but, when new data are provided to the network, the error is large. In other words, the network memorizes the training examples but do not learn to generalize new samples. A typical approach for improving generalization by avoiding overfitting is called early stopping. It consists in dividing the available data into three subsets. The first subset is the training set, which is used for updating the network weights and biases. The second subset is the validation set. The error on the validation set is monitored during the entire training process. The validation error normally decreases during the initial phase of training, as also the training error does. However, when the network begins to overfit the data, the validation error begins to rise. When it increases for a specified number of iterations, the training is stopped, and weights and biases corresponding to the minimum of the validation error are set. The test set error is not used during training, but to assess the performances of the trained network.

In the present work, as first step, days available in each dataset are randomly sorted. Then, the dataset is divided in 3 portions with equal number of days. Three ensembles of ANNs are trained: an ensemble prediction basically combines forecasts from multiple base learners to achieve improved performances, reliability and generalization capability with respect to a single base learner [22]. Each ensemble uses one of the obtained portions as test set, while the two remaining portions are merged and then the 80% of them is used as training set, while the remaining 20% is used as validation set. Each ensemble is constituted by 40 independent trials, and the independence between different trials is achieved randomly sampling the training and validation sets before each training phase. The output of the ensemble temperature estimation is equal to the median of all the single trials. Each ANN constituting the ensemble prediction takes as input the following input features: wind speed, wind direction angle, solar radiation, air temperature and current. The proposed procedure, summarized in Fig. 3, grants that the performance computed is representative of the one obtainable in a real application, because it is evaluated on the entire amount of data available.

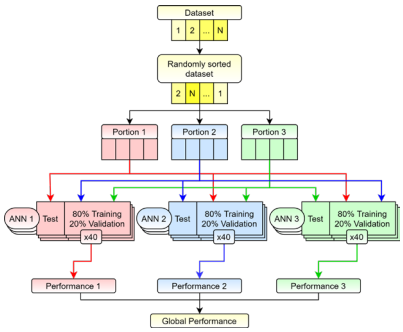

Fig. 3. Proposed ANNs procedure for line temperature estimation

Every single ANN trained presents a feed-forward architecture. Moreover, the structure presents two layers composed of hidden neurons.

Each neuron is characterized by a tan-sigmoid activation function. The selection of the number of neurons in the hidden layer is particularly important because it is directly related to the model complexity. An oversimplified network structure determines a loss of the ability to establish relations between actual and target outputs, causing underfitting issues. On the other hand, an overly complicated architecture can capture the smallest fluctuations in the training set. Hence, overfitting occurs, and the network captures even the random noise in the training set [23]. To properly establish the hidden layers size, a sensitivity analysis is carried out. In practical terms, the trade-off between performance and model complexity is studied observing the value of the network error, defined as difference between output and target quantities, in function of a variable number of hidden neurons. The result of this analysis demonstrates that the optimal network structure to be adopted with six months of data presents 12 neurons in both hidden layers. As observed before, some datasets can contain a smaller number of samples, hence a dedicated sensitivity analysis is carried out for them. The optimal network structure to work with those data presents two layers with 3 neurons each. Moreover, some of the datasets covering a six months time period presents a large number of missing days or they are heavily affected by the dataset cleaning procedure. In these cases, the described structure still constitutes a reasonable compromise between performance and complexity and is kept fixed. The network training is performed by means of an error back-propagation strategy, adopting the Levenberg-Marquardt algorithm.

III. Case Study

The performances of physical and ANN-based models are tested and compared on a case study, based on real data of several existing overhead line sections.

Data available in the present analysis are acquired by dedicated meteorological stations, installed on the line pylons (or in their surroundings). The line sections on which the conductor temperature is estimated are those next to the pylon where the weather station is installed, as depicted in Fig. 4. For the same overhead line, data from different weather stations may be available: in this case, different spans of the same line are object of analysis.

Fig. 4. Line sections considered during conductor temperature estimation

The dataset describing each line span is recorded with a 5-minutes time step and covers two different time periods, with a total duration of 7 months:

- data involved in ANN-based model training, spanning 6 months from 01/08;
- data involved in physical and ANN-based model testing, spanning for 1 month from 01/09.

Specific Line (L-) span dataset was obtained from a dedicated Weather Station (WS) located on the closest pylon of the span, namely:

- Span 1 of L-A (WS 1)
- Span 2 of L-A (WS 2)
- Span 3 of L-B (WS 3)
- Span 4 of L-C (WS 4).

Each WS is capable of measuring these data: solar radiation (W/m^2), wind speed (m/s), wind direction (°) and air temperature (°C). Besides, for each line, the average current intensity (A) is recorded. Further information on the average current flowing through each line conductor during the specified time frame is also available.

The real line temperature (°C) is also recorded, and it is employed to compare the line rating models performances. Computing the temperature output of both the ANN-based and the physical models, it is possible to estimate data deviation from the actual temperature value. Finally, the two models are compared in terms of the estimation error committed.

To achieve a proper implementation of the proposed temperature estimation model, and for a fair comparison, data clearing out of inconsistent and non-reliable samples is required. More in detail, the following exclusion criteria are applied: wind speed < 0m/s; wind direction angle < 0° or > 360°; solar radiation < 0W/m^2; air temperature > 50°C; data corresponding to sensor error alerts. On top of this preprocessing phase, datasets undertake an additional cleaning procedure consisting of a maximum wind speed value filtering. Hence, only time frames, where wind speed is lower than its mean value plus five times the wind speed standard deviation (referred to the whole available dataset), are retained in the dataset.

IV. Performance Metrics

To evaluate and compare the performance of physical and ANN-based models, three different metrics are adopted which are related on the following error formulation:

$$e_t = T^f_{line,t} - T^m_{line,t} \tag{2}$$

In the equation, $T^f_{line,t}$ and $T^m_{line,t}$ are the forecast and measured line temperature at time t, respectively.

The Mean Absolute Error (*MAE*) measures the absolute value of the mean deviation from the real value [9]:

$$MAE = \frac{\sum_{t=1}^{N}|e_t|}{N} \tag{3}$$

In the equation, N is the number of available time samples.

The Mean Bias Error (*MBE*) measures the mean of the errors committed, evaluating whether a bias in the prediction, either positive or negative, exists:

$$MBE = \frac{\sum_{t=1}^{N} e_t}{N} \tag{4}$$

Another metric adopted is the Root Mean Square Error (*RMSE*), that evaluates the dispersion degree of the forecast values around the measured quantity [9]:

$$RMSE = \sqrt{\frac{\sum_{t=1}^{N} e_t^2}{N}} \tag{5}$$

Finally, the percentage improvement allowed by ANN with respect to the temperature estimation by the physical model is computed as follows:

$$\Delta_{\%} = \frac{ERR_{Physical} - ERR_{ANN}}{ERR_{Physical}} \cdot 100 \tag{6}$$

In the equation, $ERR_{Physical}$ and ERR_{ANN} are the errors according to a certain performance metric committed by physical and ANN-based models respectively.

V. Results and Discussion

In this section, performances achieved in line temperature estimation on the test data (hence those covering the time span between 01/09 and 30/09) with the ANN-based and the physical models are compared over a time horizon of 5 minutes in advance forecast. The performance of the investigated models is computed and reported in Table II in terms of *MAE*, *RMSE* and percentage improvement.

In 3 spans out of 4 (span 1.A-1, span 2.A-2 and span 3.B-3), it is noticeable that ANNs outperform the physical models in terms of both *MAE* and *RMSE*. On these 3 spans, ANNs present an average *MAE* lower than 1°C, while physical models' estimation is characterized by average *MAE* values over 2°C. In terms of percentage improvement (Δ%), ANNs grant, on these 3 spans, a performance which is better than the physical algorithm by more than 50%. The largest improvement recorded is registered for *MAE* in span 2.A-2 and is equal to 73.1%. The only exception is represented by span 4.C-4, where the corresponding ANN shows a slight decrease in estimation accuracy in terms of *MAE* and only a

small improvement in terms of *RMSE*. On this last line, the performance levels achieved with ANN-based and physical models are yet comparable.

TABLE II.
PHYSICAL METHODS PERFORMANCE ON THE ANALYSED LINES.

MAE (°C)			
Span Line-Station	ANN	Physical	Δ%
1.A-1	0.59	2.12	72.1
2.A-2	0.96	3.57	73.1
3.B-3	0.55	1.52	63.9
4.C-4	1.91	1.82	-5.2
RMSE (°C)			
Span Line-Station	ANN	Physical	Δ%
1.A-1	0.89	2.67	66.4
2.A-2	1.39	4.41	68.5
3.B-3	0.81	2.01	59.5
4.C-4	2.12	2.46	13.7

As next step, the error distributions obtained applying ANN-based and physical models are analyzed. From theoretical point of view three possible types of error distributions are depicted as example in Fig. 5. An instance of satisfactory line temperature estimation error distribution, presenting nearly normally distributed shape with maximum concentration of the errors close to the zero value and with small weights of the distribution tails, is represented by Fig. 5(a). Fig. 5(b) depicts an error distribution which is nearly normal but unsatisfactory due to a negative bias, hence a constant tendency to underestimate the target value. Finally, in Fig. 5(c), the error distribution presents large tails, meaning that both large positive and negative error values are observed more frequently.

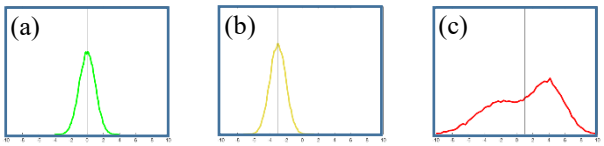

Fig. 5. Qualitative examples of error distributions: (a) Gaussian shape of satisfactory performance, (b) Gaussian shape of a biased estimation, (c) unsatisfactory performance

Fig. 6 depicts the error distributions obtained applying the ANN-based and physical models to the four spans. *MAE* and *MBE* are indicated for all the analyzed spans by a red and a black vertical lines respectively. The optimal error distribution, as shown in Fig. 5(a), is especially observed for ANNs' errors. Error distributions from physical models present shapes resembling example shown in Fig. 5(c), being quite different from a Gaussian curve. The only error distribution matching the example case displayed in Fig. 5(b) is constituted by span 4.C-4, where the distribution presents a clear bias of about -2°C of error, hence the span temperature has a constant underestimation value.

Finally, a graphical comparison is carried out in Fig. 7, where the temperature forecasts from ANNs and physical models are compared to the measured temperature for the test dataset. For the sake of the representation, comparison is shown from 11 to 14 September, but similar trends can be observed on the entire test datasets. In case of missing data, straight lines appear on the diagrams. The represented trends confirm the observation previously done on the error distributions and the improvement allowed by ANNs is visible for large regions of the diagrams. As mentioned before, the only exception is represented by span 4.C-4, where the performances of the two models are more comparable.

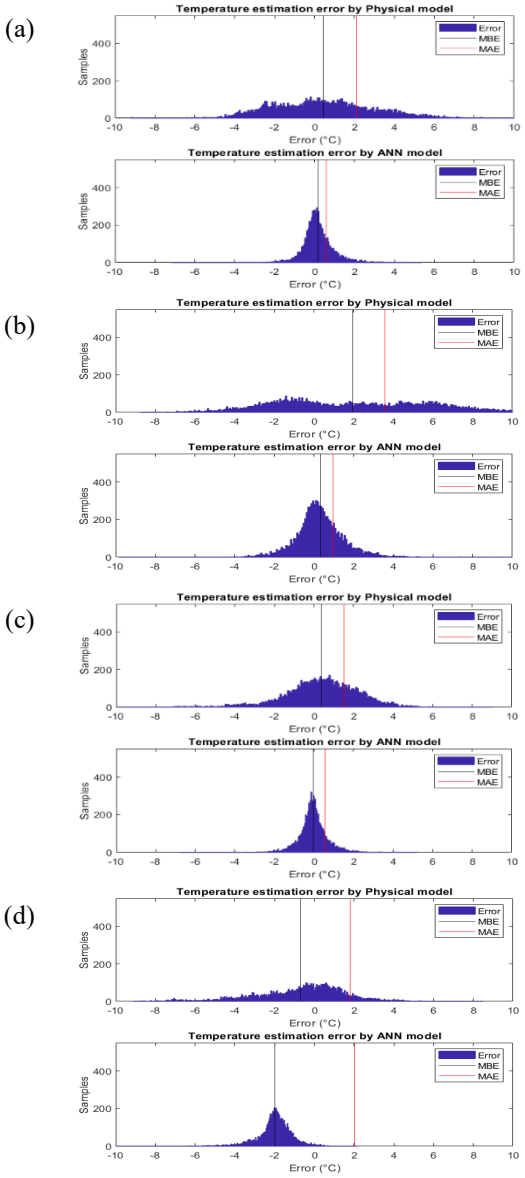

Fig. 6. Temperature estimation error of ANN and physical model of (a) Span 1.A 1, (b) Span 2.A 2, (c) Span 3.B 3, and (d) Span 4.C 4

VI. CONCLUSIONS

The aim of the present work is to compare two models for line conductor temperature estimation with a 5-minutes advance. In detail, those models are:

- ANNs (ANNs) developed with data about measured weather conditions (wind speed, wind direction, air temperature, solar radiation) and electrical current (average current flow) covering a period of six months.
- the physical algorithm usually implemented and utilized by TSOs to perform the Dynamic Thermal Rating (*DTR*).

The performances of these methods are compared on 4 real Italian overhead line sections (each one with a dedicated weather station), on a new set of data covering the period between 01/09 and 30/09. Comparison is performed in terms of error committed by each model when approximating the real temperature trend. The ANN-based approach demonstrates its superiority in terms of performance evaluated

according to specific metrics (*MAE* and *RMSE*): it grants *MAE* values generally below 1°C, corresponding to a performance improvement larger than 50% with respect to physical models, characterized by *MAE* values around 2°C.

The error distribution corresponding to ANN-based estimations resemble a normal shape centred around 0, highlighting the quality of such temperature estimation strategy. Over 4-line sections considered as a case study, only one line constitutes an exception: on that line, the performances of the two investigated methods are almost equal, with a *MAE* value (obtained with ANN) equal to 1.91°C. In light of the presented results, the optimal choice to perform a line temperature prediction with a 5-minutes forecast horizon is the approach based on ANNs, that grants an extremely accurate and flexible estimation.

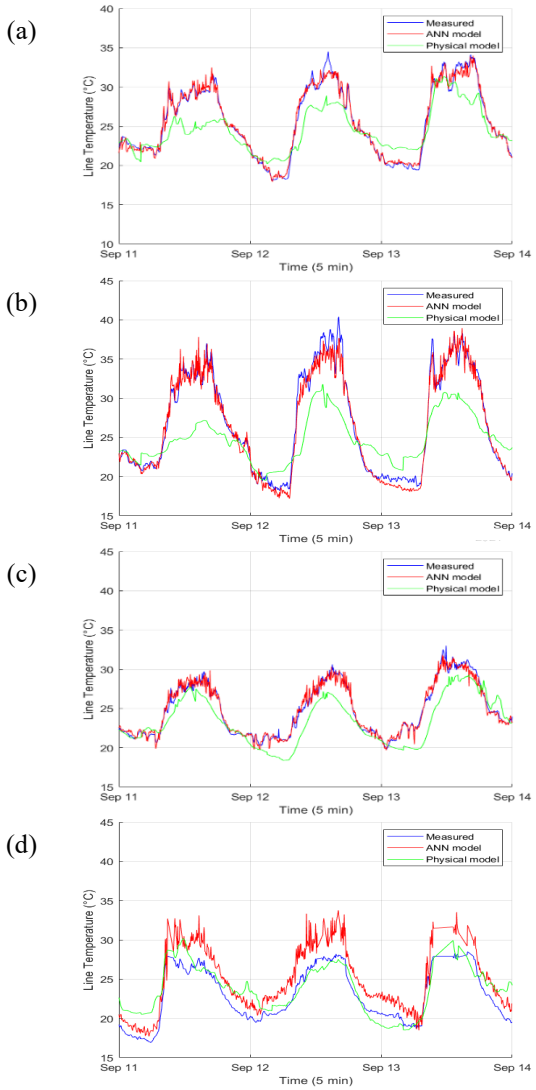

Fig. 7. Line temperature forecast comparison on three days from the test datasets: measured value (blue line), ANN estimation (red line), physical algorithm (green line) of (a) Span 1.A-1, (b) Span 2.A-2, (c) Span 3.B-3, and (d) Span 4.C-4

REFERENCES

[1] M. M. I. Bhuiyan, P. Musilek, J. Heckenbergerova, D. Koval, "Evaluating thermal aging characteristics of electric power transmission lines," Canadian Conference on Electrical and Computer Engineering, pp. 100–103, 2010.

[2] J. Teh, C. M. Lai, N. A. Muhamad, C. A. Ooi, Y. H. Cheng, M. A. A. Mohd Zainuri, M. K. Ishak, "Prospects of Using the Dynamic Thermal Rating System for Reliable Electrical Networks: A Review," IEEE Access, vol. 6, pp. 26765–26778, 2018.

[3] D. A. Douglass, J. Gentle, H. M. Nguyen, W. Chisholm, C. Xu, T. Goodwin, H. Chen, S. Nuthalapati, N. Hurst, I. Grant, J. A. Jardini, R. Kluge, P. Traynor, C. Davis, "A Review of Dynamic Thermal Line Rating Methods With Forecasting," IEEE Transactions on Power Delivery, vol. 34, no. 6, pp. 2100–2109, 2019.

[4] E. Ogliari, A. Nespoli, R. Faranda, D. Poli, F. Bassi: "Preliminary model comparison for Dynamic Thermal Rating estimation", IEEE 19th Int. Conf. on Environment and Electrical Engineering (EEEIC), Genova, Italy, pp.1-6, June 11-14, 2019.

[5] S. Bahadoorsingh, L.V. Bhairosingh, C. Sharma, "A Methodology for Dynamically Adjusting A Transmission Line Rating on an Island Grid in the Caribbean," West Indian Journal of Engineering, vol. 36, no. 2, pp. 76–83, 2014.

[6] R. Adapa, D. A. Douglass, "Dynamic thermal ratings: Monitors and calculation methods," Proceedings of the Inaugural IEEE PES 2005 Conference and Exposition in Africa, vol. 2005, no. January, pp. 163–167, 2005.

[7] CIGRE, "Guide for selection of weather parameters for bare overhead conductor ratings," Cigre Working Group, 2006.

[8] M. Beniston, D. B. Stephenson, "Extreme climatic events and their evolution under changing climatic conditions," Global and Planetary Change, vol. 44, no. 1, pp. 1–9, 2004.

[9] E. Ogliari, R. Faranda, A. Matteri, F. Bassi, M. Renieri: "Estimation of Optimal Line Angle for Dynamic Thermal Line Rating", 2021 IEEE International Conference on Environment and Electrical Engineering and 2021 IEEE Industrial and Commercial Power Systems Europe (EEEIC/I&CPS Europe), Bari, Italy, June 8-11 2021, pag. 1-5.

[10] S. Karimi, P. Musilek, A. M. Knight, "Dynamic thermal rating of transmission lines: A review," Renewable and Sustainable Energy Reviews, vol. 91, no. March, pp. 600–612, 2018.

[11] N. Siebert, "Dynamic Line Rating Using Numerical Weather Predictions and Machine Learning: A Case Study," vol. 32, no. 1, pp. 335–343, 2017.

[12] K. Morozovska, P. Hilber, "Study of the Monitoring Systems for Dynamic Line Rating," in Energy Procedia, 2017.

[13] T. O. Seppa, "Increasing transmission capacity by real time monitoring," in Proceedings of the IEEE Power Engineering Society Transmission and Distribution Conference, 2002.

[14] C. R. Black, W. A. Chisholm, "Key Considerations for the Selection of Dynamic Thermal Line Rating Systems," October, 2015.

[15] M. Blesl, A. Das, U. Fahl, U. Remme, "Role of energy efficiency standards in reducing CO2 emissions in Germany: An assessment with TIMES," Energy Policy, 2007.

[16] D. L. Alvarez, F. Faria da Silva, E. E. Mombello, C. L. Bak, J. A. Rosero, D. L. Olason, "An approach to dynamic line rating state estimation at thermal steady state using direct and indirect measurements," Electric Power Systems Research, vol. 163, pp. 599-611, 2018.

[17] J. Iglesias, G. Watt, D. Douglass, V. Morgan, R. Stephen, M. Bertinat, D. Muftic, R. Puffer, D. Guery, S. Ueda, K. Bakic, S. Hoffmann, T. Seppa, F. Jakl, C. Do Nascimento, F. Zanellato, H.-M. Nguyen, Guide for thermal rating calculations of overhead lines, 2014.

[18] A. Arroyo, P. Castro, R. Martinez, M. Manana, A. Madrazo, R. Lecuna, A. Gonzalez, "Comparison between IEEE and CIGRE thermal behaviour standards and measured temperature on a 132-kV overhead power line," Energies, vol. 8, no. 12, pp. 13660–13671, 2015.

[19] IEEE Power Engineering Society, "IEEE standard for calculating the current-temperature relationship of bare overhead conductors", IEEE Std 738-2012 pp.1-72, 23 Dec. 2013.

[20] S. Jupe, M. Bartlett, K. Jackson, "Dynamic thermal ratings: The state of the art," CIRED 21st International Conference on Electricity Distribution, no. June, pp. 6–9, 2011.

[21] I. A. Basheer, M. Hajmeer, "Artificial neural networks: Fundamentals, computing, design, and application," Journal of Microbiological Methods, vol. 43, no. 1, pp. 3–31, dec 2000.

[22] M. Aghaei, A. Dolara, F. Grimaccia, S. Leva, M. Mussetta, E. Ogliari, "PV plant planning and operations by neural network analysis and validation," 09, 2014.

[23] C. Voyant, G. Notton, S. Kalogirou, M. L. Nivet, C. Paoli, F. Motte, A. Fouilloy, "Machine learning methods for solar radiation forecasting: A review," Renewable Energy, vol. 105, pp. 569–582, 2017.